

## Evaluation of radio-immunotherapy sequence on immunological responses and clinical outcomes in patients with melanoma brain metastases (ELEKTRA)

Jessica C. Hassel<sup>a</sup>, Timo E. Schank<sup>a</sup>, Heiko Smetak<sup>b</sup>, Jasmin Mühlbauer<sup>b</sup>, Martin Salzmann<sup>a</sup>, Devayani Machiraju<sup>a</sup>, Christian Menzer<sup>a</sup>, Kristin Lang<sup>c,d</sup>, Laila König<sup>c,d</sup>, Matthias F. Haefner<sup>c,d</sup>, Ingrid Hülsmeier<sup>a,e</sup>, Christian Kohler<sup>f</sup>, Rainer Spang<sup>f</sup>, Alexander Enk<sup>a</sup>, Jürgen Debus<sup>c,d,\*</sup>, and Philipp Beckhove<sup>b,\*</sup>

<sup>a</sup>Department of Dermatology and National Center for Tumor Diseases (NCT), University Hospital Heidelberg, Heidelberg, Germany; <sup>b</sup>Regensburg Center for Interventional Immunology, University Hospital Regensburg, Regensburg, Germany; <sup>c</sup>Department of Radiation Oncology, University Hospital Heidelberg, Heidelberg, Germany; <sup>d</sup>Heidelberg Institute of Radiation Oncology (HIRO), Heidelberg, Germany; <sup>e</sup>The Immune Monitoring Unit, Deutsches Krebsforschungszentrum (DKFZ), Heidelberg, Germany; <sup>f</sup>Statistical Bioinformatics Department, Institute of Functional Genomics, University of Regensburg, Regensburg, Germany

### ABSTRACT

In patients with melanoma brain metastases (MBM), a combination of radiotherapy (RT) with immune checkpoint inhibitors (ICI) is routinely used. However, the best sequence of radio-immunotherapy (RIT) remains unclear. In an exploratory phase 2 trial, MBM patients received RT (stereotactic or whole-brain radiotherapy depending on the number of MBM) combined with ipilimumab (ipi) ± nivolumab (nivo) in different sequencing (Rad-ICI or ICI-Rad). Comparators arms included patients treated with ipi-free systemic treatment or without RT (in MBM-free patients). The primary endpoints were radiological and immunological responses in the peripheral blood. Secondary endpoints were progression-free survival (PFS) and overall survival (OS). Of 106 screened, 92 patients were included in the study. Multivariate analysis revealed an advantage for patients starting with RT (Rad-ICI) for overall response rate (RR:  $p = .007$ ; HR: 7.88 (95%CI: 1.76–35.27)) and disease control rate (DCR:  $p = .036$ ; HR: 6.26 (95%CI: 1.13–34.71)) with a trend for a better PFS ( $p = .162$ ; HR: 1.64 (95%CI: 0.8–3.3)). After RT plus two cycles of ipi-based ICI in both RIT sequences, increased frequencies of activated CD4, CD8 T cells and an increase in melanoma-specific T cell responses were observed in the peripheral blood. Lasso regression analysis revealed a significant clinical benefit for patients treated with Rad-ICI sequence and immunological features, including high frequencies of memory T cells and activated CD8 T cells in the blood. This study supports increasing evidence that sequencing RT followed by ICI treatment may have better effects on the immunological responses and clinical outcomes in MBM patients.

### ARTICLE HISTORY

Received 6 December 2021  
Revised 5 April 2022  
Accepted 11 April 2022

### KEYWORDS



Melanoma; brain metastases; radiation; immune checkpoint inhibitors; treatment sequence; immune monitoring; biomarkers

## Introduction


Almost 40–50% of advanced melanoma patients will eventually develop brain metastases which is associated with a grim prognosis.<sup>1,2</sup> The standard of care for melanoma brain metastasis (MBM) includes radiotherapy (RT) with stereotactic radiation (SRS) or whole-brain radiation (WBRT), combined with systemic therapy. Among available systemic agents, immune checkpoint inhibitors (ICIs) such as anti-CTLA4 and anti-PD1 have been shown to induce intracranial response rates comparable to those initially reported for extracranial responses.<sup>3–6</sup> Radiation therapy, through a range of diverse mechanisms, can stimulate anti-tumor immune responses, which can be enhanced by immune checkpoint inhibition.<sup>7–13</sup> RT increases tumor antigen visibility and drives immune infiltration into the tumors. Besides, RT upregulates PDL1 expression on tumor cells<sup>14</sup> and CTLA4 expression on T cells<sup>15,16</sup> which are known to downregulate immune responses and can be selectively targeted by ICIs, hence,

providing a rationale to combine RT and ICI treatments for maximum clinical benefit. In addition, there is increasing preclinical and clinical evidence for the collective effects of combining RT with ICIs.<sup>17–19</sup> However, it is unclear whether the sequence of ICI and RT (i.e., RT before ICI or ICI before RT) may influence the effectiveness of either treatment.

Systemic immune responses are required for an effective anti-tumor response to immunotherapy, especially circulating T lymphocytes are the key players in response against radiation-experienced tumor cells.<sup>20,21</sup> The combined effect of RT and ICI on peripheral T cells remains widely unclear, even though a better understanding may lead to improved patient care. Hence, this study aimed to explore the sequence of combinational treatment, i.e., RT before ICI or ICI before RT on anti-tumor and peripheral T cell responses in melanoma patients with brain metastases.

**CONTACT** Jessica C. Hassel  [jessica.hassel@med.uni-heidelberg.de](mailto:jessica.hassel@med.uni-heidelberg.de)  Department of Dermatology and National Center for Tumor Diseases (NCT), University Hospital Heidelberg, Im Neuenheimer Feld 460, Heidelberg 69120, Germany

\*These authors contributed equally to this work.

 Supplemental data for this article can be accessed on the [publisher's website](#).

© 2022 The Author(s). Published with license by Taylor & Francis Group, LLC.

This is an Open Access article distributed under the terms of the Creative Commons Attribution-NonCommercial License (<http://creativecommons.org/licenses/by-nc/4.0/>), which permits unrestricted non-commercial use, distribution, and reproduction in any medium, provided the original work is properly cited.

## Methods

### Patient selection

This is a single-center, prospective, observational, non-randomized phase 2 study with seven different patient cohorts. Patients with histologically confirmed stage IV melanoma with MRI-imaging confirmed cerebral metastases (exception: ICI control arm),  $\geq 18$  years of age and Karnofsky Performance Score  $\geq 60$ , were eligible for the study. Relevant exclusion criteria represent previous RT of the brain, patients not yet recovered from acute toxicities of prior therapies, secondary malignancy, pregnancy, and inclusion in another clinical trial. The study recruited patients between June 2013 and September 2018. Patients were followed up until data cutoff in May 2021. All patients declared written informed consent before study procedures. The study was approved by the ethical committee of the Medical Faculty of Heidelberg (S-246/2012).

### Study design

Patients were grouped into different treatment cohorts according to (i) the number of MBM and the respective choice of radiation (SRS; 1–3 lesions or WBRT; 4 or more lesions), (ii) the planned systemic treatment (ipi  $\pm$  nivo or other systemic therapy) and (iii) based on the treatment sequence (RT followed by ICI (Rad-ICI) or one cycle ICI, then RT, then ICI continuation (ICI-Rad)). There was no randomization of patients for treatment sequencing, but cohort grouping was based on the routinely planned appointments for radiation and ICI therapy (Figure 1). The main focus of the analysis was on the four cohorts of patients receiving ICI and RT in different sequencing and with either SRS or WBRT. Patients with MBM

that were planned after RT for non-ipi-based systemic therapy and patients without MBM planned for ipi  $\pm$  nivo without RT served as control cohorts, mainly for immunological analysis in the peripheral blood. Fifteen patients were planned for each treatment cohort, adding up to 105 patients. However, because of different treatment regimens (ipi  $\pm$  nivo) over recruitment was accepted to adjust.

### Treatments

#### Radiation therapy (RT)

Radiation was performed according to standard operating procedures of the Department of Radiation Oncology at Heidelberg University. SRS was applied in 1 fraction per lesion with single doses of 18–20 Gy/70–80% isodose, depending on size (volume) and location of the lesions. 3 patients received a hypofractionated radiation with 30 Gy in 6 fractions a 5 Gy as SRS in 1 fraction was not feasible. For WBRT, a total dose of 30 Gy in 3 Gy fractions or 40 Gy in 2 Gy fractions (1 patient) was applied.

#### Systemic therapy

Indication for systemic therapy was made by the Section of Dermato-Oncology of the Department of Dermatology at the National Center for Tumor Diseases, Heidelberg University Hospital, according to institutional standards. In short, patients with MBM received ipi  $\pm$  nivo (based on approval situation) either starting before (1 cycle) or after RT – depending on the time of appointment for the radiation. ICI treatment was administered with the approved doses, ipi 3 mg/kg body weight  $\pm$  nivo 1 mg/kg every three weeks for four cycles, then continued with nivo monotherapy 3 mg/kg every two weeks for

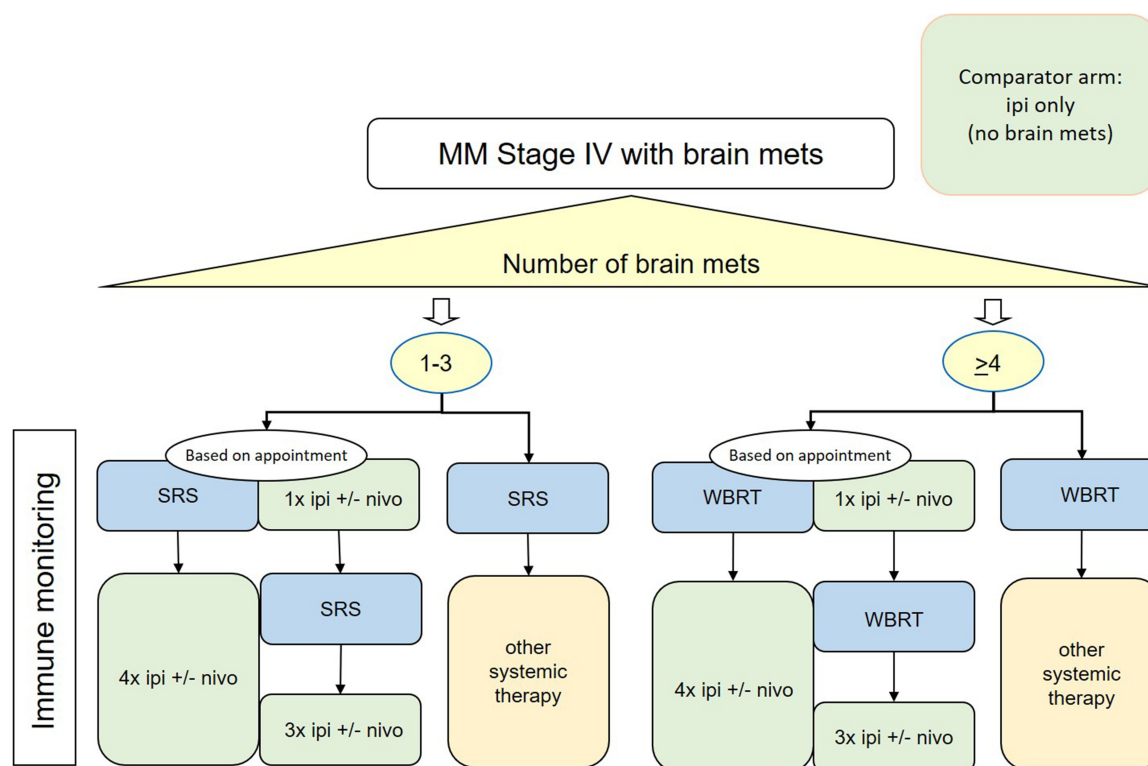


Figure 1. Flow diagram of the ELEKTRA trial.

the ipi-nivo combination group. Weekly blood draws were performed for safety. In case of severe adverse events, therapy was interrupted or discontinued based on local standard operating procedures. Patients with MBM who were ipi-experienced already and planned for another systemic treatment after RT were included in the RT control groups. All systemic therapies were continued till disease progression if the treatment was tolerated well (except ipi monotherapy with max. four cycles).

### Study endpoints

The primary endpoints were radiological tumor response according to RECIST 1.1 and systemic immunological response measured by FACS analysis of T cell subsets and Elispot against melanoma-associated antigens. Secondary endpoints were progression-free survival (PFS), and overall survival (OS).

### Assessment of tumor response and patient survival

Radiographic imaging was performed by MRI of the brain and CT of the neck, chest, and abdomen every 12 weeks from the start of ICI/RT treatment. Imaging response was evaluated in adaption to the Response Evaluation Criteria in Solid Tumors 1.1. (RECIST 1.1)<sup>22</sup>. The response rate (RR) was defined as the percentage of patients achieving a partial (PR) or complete response (CR) over the course of treatment. The disease control rate (DCR) was defined as the portion of patients achieving either stable disease (SD), PR, or CR as the best response. Secondary endpoints were progression-free survival (PFS)

and overall survival (OS), which were defined as the time from treatment start to the time of progression or death, respectively. In patients with no events of progression or death, the date of the last contact was used for censored calculation.

### Assessment of immunologic response

#### Blood sampling

For evaluation of immunologic response, 60 ml of peripheral blood was taken at baseline, before and after radiation, after 2 and 4 cycles of systemic therapy/at first staging (V1-5, Figure 2a). Pre- and on-treatment samples were collected in EDTA-coated tubes and processed according to standard NCT biobank protocols. In short, for PBMC isolation, samples were layered on top of a Ficoll-Hypaque density gradient solution (Biocoll, Biochrom). After centrifugation, the ring of PBMCs was collected, washed twice, resuspended in PBS, counted, resuspended in freezing medium (70% FCS, 20% X-VIVO 20, 10% DMSO), and frozen at  $-80^{\circ}\text{C}$  before subsequent storage in liquid nitrogen until analysis.

#### Immunophenotyping via flow cytometry

Cells washed in PBS with 2% FCS (FACS buffer) were incubated with a human Fc receptor blocking reagent (KIOVIG, 100 mg/ml infusion solution, normal human immunoglobulin, Baxter). Live/Dead cell viability dye (Thermo Fisher Scientific) was used to distinguish live and dead cells. Cells were then stained with the following extracellular fluorescent-labeled antibodies according to the T cell panel: Panel 1: CD3, CD4,

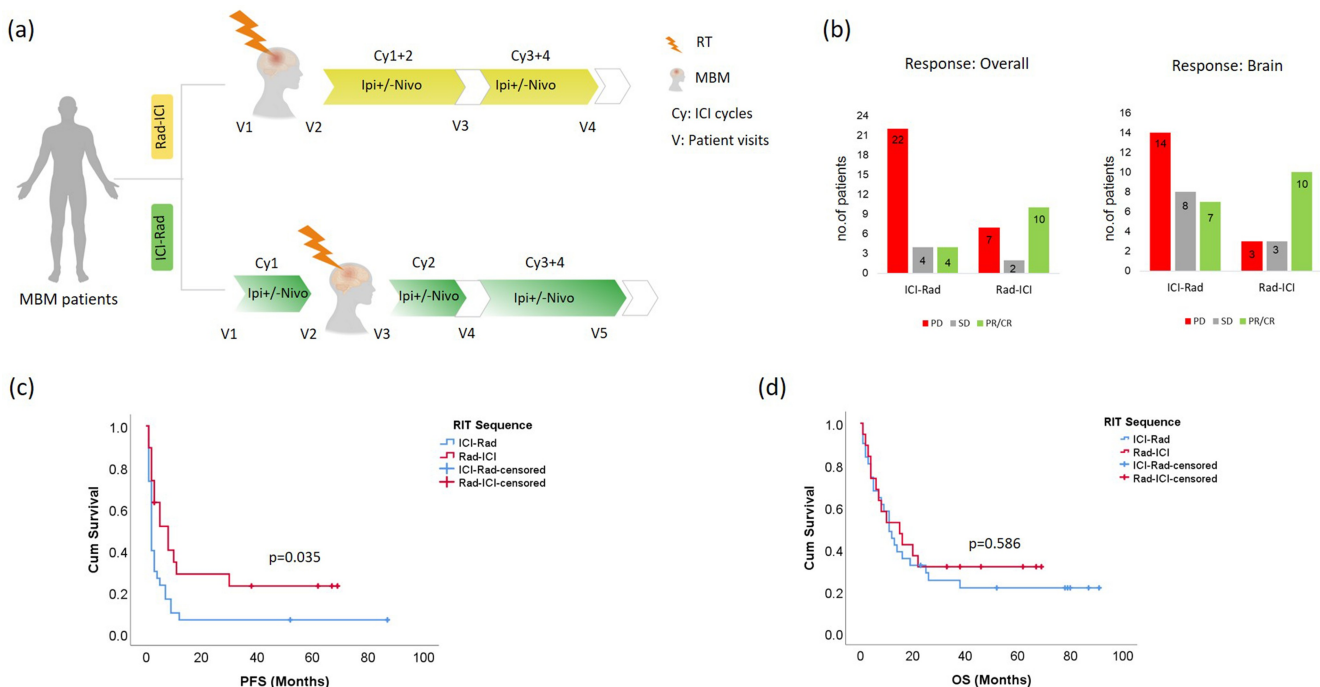


**Figure 2.** Clinical results of the ELEKTRA trial (a) Schematic representation of Radioimmunotherapy (RIT) treatment with Rad-ICI (yellow) or ICI-Rad (green) sequence in MBM patients. V1-V5 in the diagram represents study visits and displays the respective time points of immunological evaluation. (b) Overall responses (left) and intracranial responses (right) in MBM patients who received Rad-ICI or ICI-Rad treatment sequence. The red bars represent patients with disease progression (PD), gray bars represent stable disease (SD) and green bars represent a partial or complete response (PR/CR). The numbers at the top edge of the bars represent the number of patients in the respective group (c) Kaplan Meier curves for progression-free survival (PFS; left) and overall survival (OS; right) of MBM patients considering Rad-ICI (red line) or ICI-Rad (blue line) treatment sequence. p-values refer to the log-rank test.

CD25, CD127, CD45RA, or Panel 2: CD3, CD4, CD25, CD127, leukocyte alkaline phosphatase (LAP), inducible co-stimulator (ICOS) (Supplementary Table S1). Following surface staining, cells were washed twice with FACS buffer and incubated with fixation/permeabilization buffer (Invitrogen) at 4°C for 30 minutes. Cells were then washed in permeabilization buffer and were intracellularly stained for FoxP3 and Ki67 (Panel 1) or FoxP3 alone (Panel 2) for 30 minutes at 4°C. After washing, the cells were analyzed on a BD FACS Canto II (BD Biosciences) with single-stained antibody-capturing beads used for compensation (CompBeads, BD Biosciences). Data were analyzed using FlowJo software version 10 (Tree Star, Ashland, OR, USA).

### *IFN-gamma elispot analysis*

The quantitative evaluation of antigen-specific T cells secreting interferon- $\gamma$  (IFN- $\gamma$ ) was performed as described previously<sup>23</sup> with modifications. After thawing and overnight rest, the average yield of viable cells, as determined by Trypan blue (Sigma Aldrich) viability staining, amounted to 66%. Thawed PBMCs were cultured for 2 hours, after which non-adherent cells were washed off and cultured in X-VIVO 20 medium (Biolyon) supplemented with 100 U/ml interleukin (IL)-2 (Novartis) and 60 U/ml IL-4 (Miltenyi Biotec). The adherent cells were cultured with 560 U/ml of recombinant human granulocyte monocyte colony-stimulating factor (GM-CSF) (Genzyme) and 500 U/ml IL-4 (Miltenyi Biotec). One day ahead of purification (after 6–7 days of culture), both cell fractions were cultured in cytokine-free media (X-VIVO 20, Biolyon). Dendritic cells were enriched by negative selection using the Pan Mouse IgG Dynabeads (Thermo Fisher Scientific), coupled to mouse anti-human CD56 (clone: C218, Beckman Coulter) as well as CD3 and CD19 Dynabeads (both Thermo Fisher Scientific). T cell purification was performed using the Untouched<sup>TM</sup> Human T Cell system (Thermo Fisher Scientific). ELISpot plates (Human IFN- $\gamma$  ELISpot PLUS (ALP), Mabtech) were blocked, with complete RPMI medium (Sigma), containing 10% FCS (Biolyon), for 30 minutes at room temperature. Dendritic cells were plated in triplicates and loaded with 10 mg/ml of five melanoma-associated antigenic peptides, each<sup>24</sup> (Melan-A, Tyrosinase, Na17A, p53, MDM2) and a pool of all 5, all of which embed described immunogenic HLA-A2-restricted epitopes as indicated in supplementary table S2 and likely to contain several epitopes restricted to other HLA-I and -II-alleles as predicted by common public databases. All test peptides were produced by the Peptide Synthesis Facility of the DKFZ. Lyophilized synthetic 50 amino acid long peptides were solved in distilled water containing 10% DMSO. Peptide purity was >98%. A pool of the pp65 protein of human cytomegalovirus (PepTivator CMV pp56, Miltenyi Biotec), mixed with the hexon protein of human adenovirus 5 (PepTivator AdV5 Hexon, Miltenyi Biotec), as well as PHA (Lectin from phaseolus Vulgaris, Sigma-Aldrich), were used as positive controls. Human Normal Immunoglobulin (KIOVIG, Baxter) was used as a negative control. After 14 h of antigen pulsing, purified T cells were added to each well in a 5:1 ratio for an additional 46-h co-culture. IFN $\gamma$  spots were developed using an enzyme-coupled detection antibody system utilizing a biotinylated anti-

IFN $\gamma$  antibody (clone 7\_B6-1 diluted 1:1000, Mabtech), streptavidin ALP (diluted 1:1000, Mabtech), and NCT/BCIP substrate kit (Mabtech). Plates were analyzed using an automated ELISpot reader and ImmunoSpot Software V 5.0 (CTL Europe) using the following settings: Minimum Spot size 0.0051 mm<sup>2</sup>; Maximum Spot Size: 9.6466 mm<sup>2</sup>; Spot Separation: 3; Diffuse Processing: normal; Background Balance: 0–80. Wells with too many spots (too numerous to count – TNTC) were defined as 800 spots. Individuals were considered responders if the spot numbers in the triplicate test wells significantly (two-tailed t-test with  $p < .05$ ) exceeded the numbers in the negative control.

### *Statistical analysis*

Chi-square test and MWU-test were used to compare the differences in clinicopathological characteristics of patients among the Rad-ICI and ICI-Rad sequence groups. Differences between the clinical variables and treatment response were assessed by univariable regression analysis. As this is a non-randomized trial, multivariable regressions were performed to adjust for potential confounders based on univariable regression analysis. Only baseline variables that achieved a significance level of  $p < .05$  in the univariate analysis were included in the multivariate model. Kaplan–Meier analysis and the log-rank test were used for survival analysis, and the hazard ratio (HR) was determined through a Cox proportional hazard regression model. The dynamics of peripheral T cell subsets at different time points of treatment were analyzed using paired T-test, whereas the kinetics and magnitude of tumor antigen-specific T cells in the blood were analyzed using two-way ANOVA.  $p$  values were considered significant with values of  $p < .05$ . All statistical analyses were performed using IBM SPSS Statistics (version 26) and GraphPad Prism 8 (version 8).

### *Predictive modeling with LASSO*

A logistic Lasso regression analysis was performed to analyze the impact of different immunological parameters on predicting the remission or progression of patients. Evaluable data for analysis of immunologic response consisted of 256 samples from 76 individuals with visits ranging from 1 to 5. Every sample is characterized by 47 different immunological markers and 11 clinical features (Supplementary Table S3). A logistic LASSO regression model for binary class prediction (progression or non-progression) was trained as implemented in the R package glmnet (version 3.0–2).<sup>25</sup> We predicted clinical responses for the features of all visits separately and combined them using majority voting to obtain a single prediction per patient. LASSO regression involves a shrinkage parameter that calibrates overfitting-reducing L1-regularization. To tune  $\lambda$ , we use Leave-One-Out Cross-Validation to find the value  $\lambda_{\min}$ , which minimizes the cross-validation prediction error. The corresponding model for  $\lambda_{\min}$  was then used to predict clinical outcomes in all patients, again in Leave-One-Out Cross-Validation. Seven individuals, each with data from two visits only, were labeled as “ties” as majority vote prediction was not unique. This resulted in a prediction accuracy of 75.4%, suggesting that clinical and immunological markers predict the outcome. Beyond prediction of outcome, LASSO regression

trained on all samples identified the small subset of features that allowed for the prediction. Moreover, it scored every feature according to its impact on prediction. Features with positive scores *S* are associated with progression, whereas features with negative scores are associated with non-progression. All further statistical analyses were performed using the free software R (Version 3.6.2).<sup>26</sup>

## Results

### Patient characteristics

In total, 106 patients were recruited in this trial with a median age of 61 years, 71% male. Of these, 14 patients (13%) were screen failures (Supplementary Fig. 1). 42/92 (46%) revealed up to 3 MBM and received SRS, 29/92 (32%) had at least 4 MBM and received WBRT, 21/92 (23%) were included without MBM and did not receive any RT (control group "ICI" no MBM). During the course of the trial, the approval status changed from ipi monotherapy to ipi-nivo combination therapy. Mainly based on this, 42/92 (46%) of patients received ipi monotherapy and 30/92 (33%) ipi-nivo combination therapy. 20/92 (22%) of patients received RT, either SRS or WBRT, without ipi-based systemic therapy (control group "Rad"). Here, the group was heterogeneous with 6/92 (7%) receiving anti-PD-1 monotherapy, 6/92 (7%) BRAF/MEK inhibition, 2/92 (2%) dacarbazine chemotherapy, 1/92 (1%) MEK inhibitor monotherapy, and 5/92 (5%) without any systemic treatment after RT. Of the 50 patients receiving both RT and ipi, 19 started with RT (38%, "Rad-ICI" group), and 31 started with ipi-based ICI (62%, "ICI-Rad" group) (Supplementary Fig.1; Figure 2a). For exploratory efficacy analysis, these two groups receiving both RT and ipi-based immunotherapy (RIT) were included. The median interval between the start of radiation and initiation of ICI treatment was 19 days (95% CI: 13–22) in the Rad-ICI group and 10 days (95% CI: 8–14) in the ICI-Rad group.

Because this was a non-randomized observational trial, the RIT treatment groups were analyzed for differences in patients' baseline characteristics (Table 1).

Significantly, more patients in the Rad-ICI group received ipi+nivo combination therapy (58%) compared to the ICI-Rad group ((19%);  $p = .005$ ). Furthermore, there was a tendency of patients receiving more often ipi+nivo combination therapy in the WBRT group (46%) than in the SRS group ((23%);  $p = .090$ ). Hence, patients with the ipi-nivo combination started more often with radiation and tendentially received more often WBRT because of at least 4 MBM.

### Radiological response and survival of RIT sequence treatments

Univariate analysis revealed better overall response rates (RR) and disease control rates (DCR) in patients who started with RT and then received ipi ± nivo (Rad-ICI: RR 53% and DCR 63%) compared to the patients who started with one cycle of

**Table 1.** Clinical baseline characteristics and treatment outcomes of MBM patients treated with radiation and immunotherapy (RIT) sequences.

	MBM Patients with RIT Sequence (50) n (%)		
	Rad-ICI (19)	ICI-Rad (31)	p-value
Clinical characteristics			
Age (Median)			
< 61 Years	9 (47)	15 (48)	0.944
> 61 Years	10 (53)	16 (52)	
Gender			
Male	15 (79)	22 (71)	0.532
Female	4 (21)	9 (29)	
LDH			
Elevated	5 (26)	12 (39)	0.369
Normal	14 (74)	19 (61)	
Prior Systemic treatment			
Yes	3 (16)	7 (23)	0.560
No	16 (84)	24 (77)	
Type of Radiation			
SRS	8 (42)	18 (58)	0.273
WBRT	11 (58)	13 (42)	
Type of ICI			
Ipilimumab	8 (42)	25 (81)	0.005
Ipilimumab + Nivolumab	11 (58)	6 (19)	
Clinical outcome			
Response Brain			
PD	3 (16)	14 (45)	0.035
SD	3 (16)	8 (26)	
PR/CR	10 (53)	7 (23)	
NA	3 (16)	2 (6)	
Response Overall			
PD	7 (37)	22 (71)	0.011
SD	2 (10)	4 (13)	
PR/CR	10 (53)	4 (13)	
NA		1 (3)	
irAEs			
Yes	7 (37)	14 (45)	0.563
No	12 (63)	17 (55)	
PFS (Months)			
Median (95% CI)	5 (2–30)	2 (2–3)	0.019
OS (Months)			
Median (95% CI)	15 (4–38)	11 (5–23)	0.834

ICI followed by RT (ICI-Rad: RR 13% and DCR: 26%)(RR:  $p = .005$ ; HR: 7.22 (95%CI: 1.81–28.8); DCR:  $p = .01$ ; HR: 4.71 (95% CI: 1.37–16.2))(Figure 2b; Table 2). However, as the Rad-ICI group consisted of more patients with ipi-nivo combination therapy than the ICI-Rad group (Table 1), this effect might have just been based on the systemic treatment regimen. Matching to this, patients receiving combination ICI therapy achieved a numerically better RR ( $p = .11$ ) and significantly better DCR ( $p = .042$ ) than patients with ipi monotherapy. Therefore, multivariate analysis was performed, which demonstrates that the Rad-ICI sequence remains a significant factor associated with better responses (RR and DCR) when adjusted for potential confounding factors such as ICI regimen and tumor load measured by serum lactate dehydrogenase (LDH) ( $p < .05$ ; Table 2).

Accordingly, intracranial response rates (defined for the whole brain and not only for the irradiated metastases) were higher in patients who received the Rad-ICI treatment sequence (RR 53% and DCR 68%) compared to the group of patients who received the ICI-Rad sequence (RR 23% and DCR 48%) (RR:  $p = .014$ ; HR: 5.24 (95%CI: 1.40–19.65); DCR:  $p = .059$ ; HR: 4.04 (95%CI: 0.95–17.27)) (Figure 2b); Supplementary Table S4). Apart from the RIT

**Table 2.** Univariate and multivariate analysis for overall responses in RIT treated MBM patients.

Overall Response Rate (RR)				
Parameters	Univariable Regression		Multivariable Regression	
	HR (95% CI)	p	HR (95% CI)	p
<b>Age</b>				
(<61 Vs >61 Years)	0.42 (0.12–1.50)	0.181		
<b>Gender</b>				
(Male Vs Female)	0.42 (0.08–2.21)	0.303		
<b>Prior Systemic Treatment</b>				
(No Vs Yes)	1.09 (0.24–5.0)	0.911		
<b>LDH</b>				
(Normal Vs Elevated)	0.10 (0.01–0.87)	0.037	0.09 (0.01–0.88)	0.038
<b>Type of ICI Treatment</b>				
Ipi Vs IpiNivo	2.89 (0.79–10.5)	0.108		
<b>Type of Radiation</b>				
SRS Vs WBRT	1.19 (0.34–4.11)	0.786		
<b>irAEs</b>				
No Vs Yes	1.69 (0.48–5.92)	0.410		
<b>RIT Sequence</b>				
ICI-Rad Vs Rad-ICI	7.22 (1.81–28.8)	0.005	7.88 (1.76–35.27)	0.007
<b>Overall Disease Control Rate (DCR)</b>				
<b>Age</b>				
(<61 Vs >61 Years)	0.33 (0.1–1.0)	0.07	0.19 (0.04–1.02)	0.053
<b>Gender</b>				
(Male Vs Female)	0.66 (0.17–2.57)	0.55		
<b>Prior Systemic Treatment</b>				
(No Vs Yes)	0.96 (0.23–3.95)	0.95		
<b>LDH</b>				
(Normal Vs Elevated)	0.12 (0.02–0.61)	0.01	0.07 (0.01–0.49)	0.008
<b>Type of ICI Treatment</b>				
Ipi Vs IpiNivo	3.83 (1.09–13.45)	0.04	1.66 (0.3–9.3)	0.562
<b>Type of Radiation</b>				
SRS Vs WBRT	0.88 (0.28–2.75)	0.82		
<b>irAEs</b>				
No Vs Yes	1.34 (0.42–4.26)	0.62		
<b>RIT Sequence</b>				
ICI-Rad Vs Rad-ICI	4.71 (1.37–16.2)	0.01	6.26 (1.13–34.71)	0.036

sequence, the response rates in the brain were significantly better in patients who received ipi-nivo combination therapy (RR:  $p = .042$ ) compared to ipi monotherapy and in patients with normal LDH (RR:  $p = .041$ ). However, we did not observe any significant impact of the type of radiation patients received on intracranial responses (RR:  $p = .465$ ; DCR:  $p = .609$ ), having in mind that patients with WBRT had more brain metastases. In multivariate analysis, however, the RIT sequence remained the only significant factor for both intracranial RR and DCR ( $p = .092$  and  $p = .098$ , respectively) (Supplementary Table S4).

Concerning patient survival, the patient group treated by the Rad-ICI sequence experienced a significantly better progression-free survival (PFS) compared to patients treated by the ICI-Rad sequence ( $p = .035$ ; HR: 2.02 (95% CI: 1.0–3.88); Figure 2c). RIT sequence remained a trending factor associated with PFS when adjusted for ICI treatment ( $p = .162$ ; HR: 1.64 (95% CI: 0.8–3.3)(Supplementary Table S5). However, there was no difference in overall survival (OS) between the groups ( $p = .586$ , HR: 1.207 (95% CI: 0.614–2.371); Figure 2d).

## Immunological response of RIT sequence treatments

Immune monitoring included the analysis of T cell subsets in the peripheral blood using Flow cytometry (FACS) at several time points from baseline till the first staging 12 weeks after treatment initiation (V(visit)1–V5, Figure 2a). Results from the FACS analysis showed that after the first cycle of ipi-containing ICI treatment, a temporarily significant increase ( $p < .05$ ) in the frequencies of activated T cells measured by the proliferation marker Ki67, and the activation marker ICOS (CD45RA-Ki67 + CD4+, CD45RA-Ki67+ CD8+, ICOS+CD4+, and ICOS+CD8+) was detectable, including regulatory T cells (Tregs; CD3+ CD4+ CD25+ CD127-FOXP3+) (Supplementary Fig. 2). Interestingly, although we noticed WBRT tendency to reduce the total number of circulating lymphocytes in the blood (Supplementary Fig. 3), similar to ipi, we observed an increase in activated lymphocytes upon WBRT (Supplementary Fig. 2). However, in line with a previous report<sup>27</sup> we found no differences in peripheral immune responses upon SRS. After two cycles of ICI treatment in both Rad-ICI and ICI-Rad treatment groups, the frequencies of CD45RA-Ki67+ and ICOS+ subsets of CD4 and CD8 T cells remained elevated compared to baseline, irrespective of radiation modality ( $p < .05$ ; Figure 3a–f; timepoint after two cycles of ICI = V4 in ICI-Rad group and V3 in Rad-ICI group (compare Figure 2a)). At this time point, we also observed an increase in the frequencies of activated Ki67+ Tregs in the ICI-Rad group ( $p = .037$ ) but not in the Rad-ICI group ( $p = .230$ ; Figure 3e), conversely, an increase in circulating CD8 T cells (%CD3+ CD4-) was observed in the Rad-ICI group ( $p = .009$ ), but not the ICI-Rad group ( $p = .702$ ; Supplementary Figure 4). At the time of first follow-up imaging after three months, there was a significant increase in the frequencies of CD45RA-CD4-Ki67+ (CD8) and CD3+ CD4+ ICOS+ (CD4) T cells in the Rad-ICI group ( $p = .049$  and  $p = .016$ ) but not in the ICI-Rad group ( $p = .386$  and  $0.537$ ; Figure 3b, c). However, it is important to remember that more patients received ipi-nivo combination therapy in the Rad-ICI group than the ICI-Rad group. Therefore, a comparison between systemic therapy modalities (ipi monotherapy vs. ipi-nivo combination) within the ICI-Rad and Rad-ICI groups was performed and revealed a transient increase of activated Tregs after two cycles of ipi monotherapy within the Rad-ICI group (Supplementary Fig. 5 f). In contrast, significantly more activated CD4 and CD8 T cells (Supplementary Fig. 5b, d) were found three months after treatment initiation at the time point of the first follow-up imaging in the Rad-ICI group when ipi-nivo combination therapy was applied. The sample sizes were too small to compare the immune profile between responders and non-responders in the respective groups.

ELISpot analysis to test for T cell reactivity against melanoma-specific antigens revealed a significant increase in tumor-antigen specific reactivity of IFN- $\gamma$  secreting T cells following radiation and after two cycles of ICI in both the Rad-ICI ( $p < .01$ ; Figure 4a) and the ICI-Rad ( $p < .05$ ; Figure 4b) groups. This increase was consistently found in patients with partial or complete remission ( $n = 7$ ) or stable disease ( $n = 1$ ) but not in patients with disease progression ( $n = 4$ ) (Supplemental Figure. 6). Although not statistically significant,

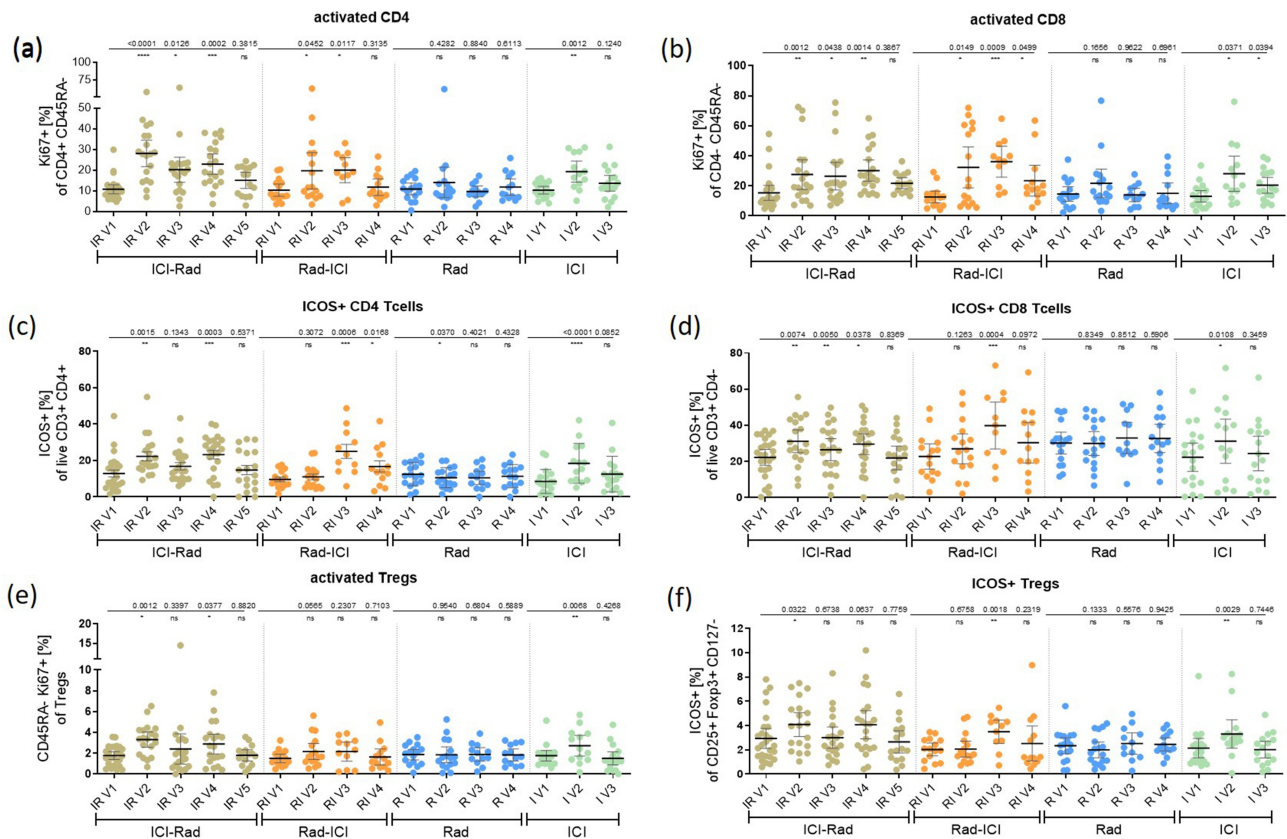


**Figure 3.** Longitudinal analysis of circulating T cell subsets plotted as the percentage of live single CD3 + T cells (a) activated CD4+ cells (b) activated CD8+ cells (c) ICOS+CD4+ cells (d) ICOS+CD8+ cells (e) activated Tregs (f) ICOS+Tregs. V1-V5 in the graphs represents the respective time points of immunological evaluation, as shown in Figure 2a. V1: baseline; V2: after the first dose of ICI (ICI-Rad) or after radiation (Rad-ICI); V3: after radiation (ICI-Rad) or after 2 cycles of ICI (Rad-ICI); V4: After two cycles of ICI (ICI-Rad) or after imaging (Rad-ICI); V5: after imaging (ICI-Rad). Each dot represents a measured value from a single patient at the given time point. The lines represent the mean with upper and lower 95% confidence intervals. Statistical comparisons between time points were made using the paired T-test. p-values < 0.05 were considered significant (\*\*\*\*p < .0001, \*\*\*p < .01, \*p < .05). ns stands for no statistical significance.

the same trend of increased antigen reactivity was observed in the Rad group at the corresponding time point (Figure 4c). However, we did not observe any such activity in the ICI alone group (Figure 4d). Interestingly, at the time of imaging, T cell reactivity significantly decreased in the Rad-ICI and Rad groups but not in the ICI-Rad and ICI groups (Figure 4). Overall, pooled virus-specific memory T cell frequencies followed a similar, though less pronounced kinetic as pooled tumor antigen-specific ones.

### Clinical and blood parameters associated with treatment outcome

Lasso regression analysis revealed the impact of different clinical and T cell parameters on disease control versus disease progression on the prediction of outcome in melanoma patients (Figure 5 and supplementary table S3). Among them, we found that the treatment with ipi monotherapy ( $S = 0.493$ ), the extent of change in the number of activated Tregs over baseline Tregs ( $S = 0.484$ ), ICI-Rad treatment sequence ( $S = 0.477$ ), and the frequency of Tregs (CD25+ FoxP3+;  $S = 0.469$ ) had the greatest influence on the prediction of disease progression. Whereas, anti-PD1 treatment ( $S = -0.889$ ), the frequency of memory T cells (CD45RA-;  $S = -0.558$ ), the Rad-ICI treatment sequence ( $S = -0.467$ ), and the rate of change in the number of activated CD8

T cells over baseline Tregs ( $S = -0.465$ ) were the most predictive parameters associated with disease control. A difference in the frequencies of peripheral T cell subsets according to the response could be detected early after two cycles of ICI treatment. Higher frequencies of CD8 memory T cells ( $p = .012$ ; Figure 5b) and a striking increase in activated CD8 memory T cells and ICOS+ CD8 T cells after two cycles of ICI treatment were noticed in disease control patients ( $p < .0001$  and  $p = .001$ ; Figure 5c, d). At the same time, an increase in activated CD4 + Treg cells was seen in patients with disease progression ( $p = .0096$ ; Figure 5e).

### Discussion

The main goal of our prospective trial was to explore immunologic parameters in MBM patients treated with different treatment sequencing of ipi ± nivo and radiation and investigate clinical outcomes. In addition, we recruited patients with different numbers of brain metastases to find differences between SRS and WBRT in the interaction with ICI therapy. Our study further supports growing data that for advanced melanoma patients with brain metastases, a sequence of combination treatment starting with radiation followed by ipi-based ICI treatment (Rad-ICI) might result in better responses and PFS than the sequence starting with ICI followed by radiation (ICI-Rad). This was corroborated by immunological

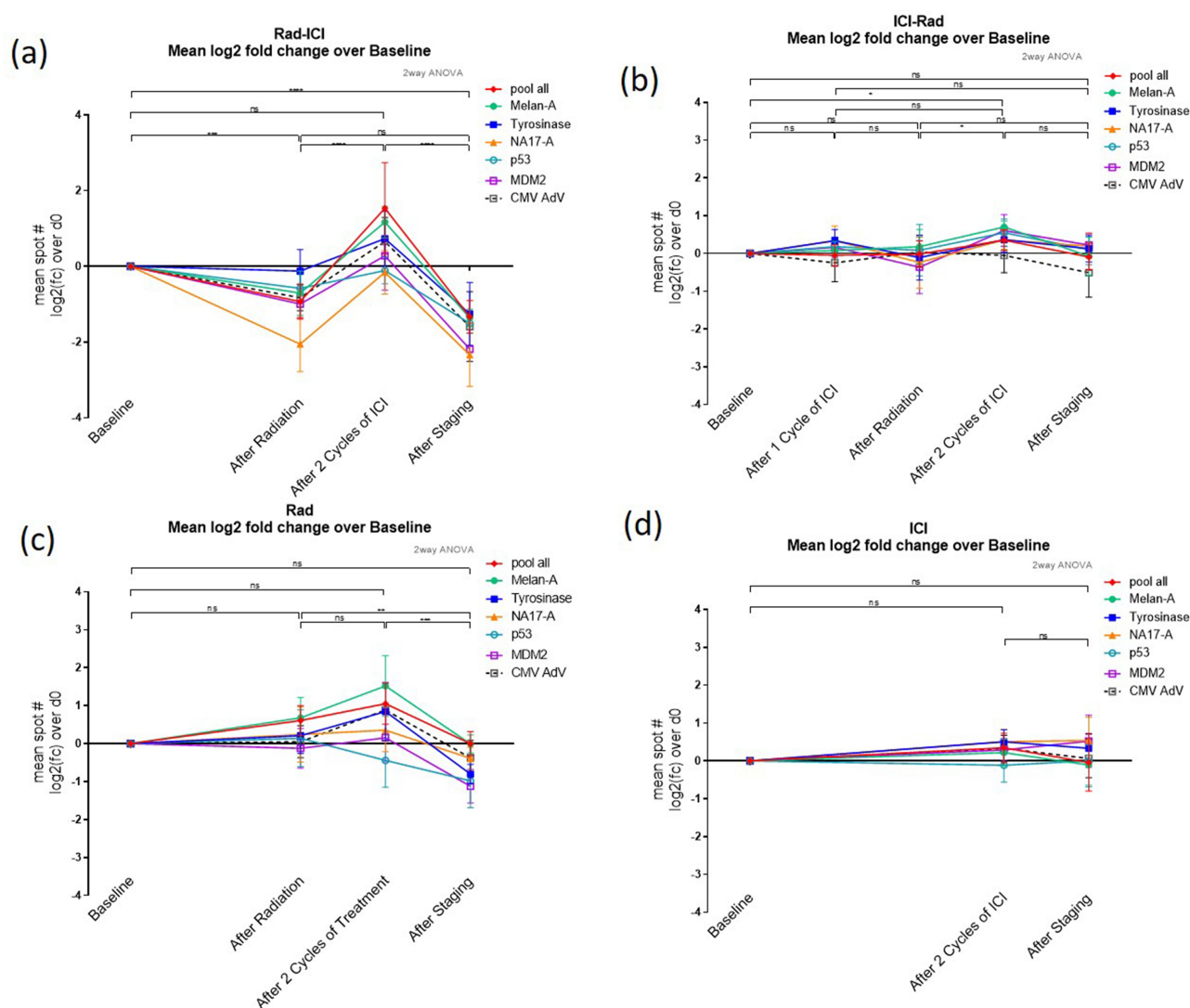


**Figure 4.** Longitudinal monitoring of IFN $\gamma$  ELISpot responses to tumor-specific antigens. The magnitude of IFN $\gamma$  ELISpot responses to 5 tumor-related proteins (Melan-A, Tyrosinase, NA17-A, p53, MDM2) at indicated times during the treatment (a) Rad-ICI (b) ICI-Rad (c) Rad (d) ICI, expressed as log fold change in the average of spot-forming cells (SFC) over baseline values. Statistical comparisons between indicated time points were made using the two-way ANOVA. The lines represent the mean with the standard error of mean. p-values < 0.05 were considered significant (\*\*\*\*p < .0001, \*\*\*p < .001, \*\*p < .01, \*p < .05). ns stands for no statistical significance.

data showing that especially in the Rad-ICI group ipi-nivo combination therapy leads to a significant increase in activated CD4 and CD8 T cells in the peripheral blood. Even though ipi leads to an increase in activated CD4 and CD8 T cells in all groups, ELISpot analysis showed that patients with clinical remission or stable disease after treatment with a combination of RT and ICI therapy developed a transient increase in T cell reactivity against melanoma antigens which was not significant in patients treated with ICI alone. This transient increase in responding patients must be interpreted with caution as the underlying data are derived from a few patients only, and potential causes can only be speculated. On the one hand, activation and proliferation of melanoma-reactive T cells can be boosted by ICI treatment as this removes inhibitory signals upon antigen recognition, finally supporting tumor remission. Subsequent reduction of melanoma reactive T cells could thus result from i) the omission of the ICI stimulus and/or ii) from a reduced antigen load due to tumor shrinkage. On the other hand, recent studies in models of

chronic viral infection suggest that PD1 blockade may also cause long term adverse effects on the memory T cell pool: while exhausted T cells regain function after PD1 inhibition, the pool of earlier induced resting, antigen-specific memory CD8 T cells decreased.<sup>28</sup> The latter hypothesis is supported by our observation that virus-reactive T cells diminished after ICI therapy to a higher degree than tumor antigen reactive ones in responding patients.

Several preclinical and clinical studies have demonstrated promising synergy between RT and ICI.<sup>17-19</sup> However, for the design of beneficial Radio-Immunotherapy (RIT), the appropriate timing of RT and ICI might be important to optimize treatment response.<sup>29-35</sup> Kiess et al. investigated 46 patients with MBM who received SRS during, before, or after ipi treatment. OS seemed to be better if the RT was done before or under ipi therapy compared to RT after ipi. However, RT after ipi most likely occurs because of disease progression in the brain, and this result might therefore just correlate with ipi resistance.<sup>29</sup> Ipi resistance is also likely to be the reason for



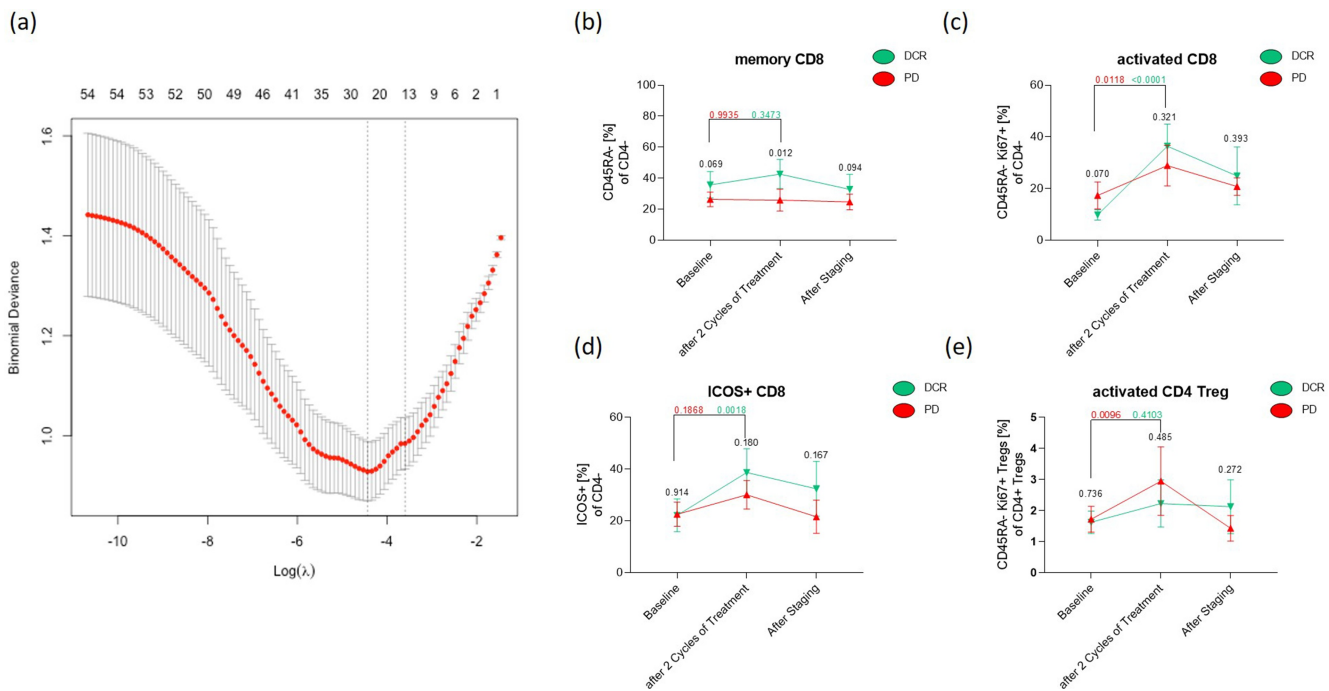


**Figure 5.** Clinical and T cell parameters associated with treatment response. (a) Cross-Validation plot for Lasso regression (Lambda path for all  $n = 58$  features). The plot displays the Cross-Validation error according to the log of the shrinkage parameter  $\lambda$ . The dashed lines indicate the log  $\lambda$  values corresponding to the  $\lambda_{\min}$  (left dashed line) and  $\lambda_{1se}$  (right dashed line).  $\lambda_{\min}$  represents the value for which the model yields the lowest cross-validation mean squared error, hence minimizing the prediction error. The numbers on top represent the number of non-zero regression coefficients in the model (= the number of included features). From left to right along the x-axis, with increasing  $\lambda$ , fewer variables are included in the model since the penalty for inclusion of features is weighted more heavily. In other words: the log( $\lambda$ ) value at  $\lambda_{\min}$  corresponds to the most accurate model with the best predictive ability and the optimal/sparse set of features ( $n = 24$ ). (b-e) Comparisons between T cell subsets (b) memory CD8 cells (c) activated memory CD8 cells (d) ICOS+ CD8 cells (e) activated Tregs at different time points in patients with progressive disease (PD) or disease control (DCR). The difference in the means of PD and DCR groups was assessed using an unpaired t-test, and p values were corrected for multiple comparisons using the Holm-Sidak method. The difference between the two-time points (baseline vs. two ICI cycles) was performed using 2-way ANOVA (Turkey's Multiple comparisons test). Adjusted p values were labeled on the top of the graphs (red for progression and green for disease control). The lines represent the mean with the standard error of the mean. p-values  $< 0.05$  were considered significant.

a worse clinical outcome with the sequence ipi-RT in another retrospective analysis<sup>34</sup> as the time interval from ipi to RT was up to 21 months, hence probably at disease progression. Similarly, in a case review of 16 patients who received WBRT plus SRS with ipi, it was found that receiving SRS before ipi was associated with improved survival compared with receiving ipi first.<sup>31</sup> In another study, improved OS was observed among MBM patients who started ipi within 14 days after SRS compared to those who started ipi therapy later<sup>32</sup> suggesting the close temporal proximity of this sequence is most important for maximal efficacy. This goes in line with our positive results of the Rad-ICI group, where ipi  $\pm$  nivo treatment was started at a median of 19 days after RT. However, we only found a benefit in intracranial and overall response rates as well as progression-free survival but not overall survival for the sequencing starting with radiation compared to the ICI-Rad sequence. In both groups, an increase in tumor antigen reactivity of IFN- $\gamma$  secreting T cells, suggesting an increase of more specifically tumor-reactive T cells, was found after the second ipi  $\pm$  nivo cycle. At the time of first tumor imaging three months after treatment start, the observed reduction in tumor antigen reactivity of IFN- $\gamma$  secreting T cells was accompanied by an increase in ICOS+CD4 + T cells compared to baseline in the Rad-ICI group but not in the ICI-Rad group. It was previously shown that the ICOS pathway is required for optimal anti-tumor responses mediated by anti-CTLA4 therapy, and hence

increased numbers of these cells might indicate the enhanced efficacy of anti-CTLA4 in this group.<sup>36</sup> Collectively, the overall weight of evidence supports the framework that the efficacy of the combination of therapies is likely optimized when given the sequence starting with radiation followed by ipi-based ICI (Rad-ICI) with relatively close proximity. This may be due to radiating tumors before ICI treatment may increase the antigen presentation and prime tumor-specific T cells, which can be effectively reactivated by ICI treatment upon exhaustion. Whereas, with the ICI-Rad sequence, the tumor-specific immune responses activated by ICI treatment may have been hampered by the immunosuppressive effect of the following RT leading to the reduced clinical responses observed in this group. In addition, the application of ICI after RT might foster a potential abscopal effect of the RT. In line with this, in a lung cancer trial PFS and OS rates were improved in patients who had received photon radiotherapy prior to immunotherapy.<sup>37</sup> However, it is important to note, that different sites of radiation might have different effects. In an investigation of 40 patients with solid tumors an increase in activated memory CD4 and CD8 T cells was only seen after SRS to parenchymal sites and not to bone and brain.<sup>27</sup> Larger clinical trials are required to verify these findings, especially involving anti-PD1 therapy. This accounts not only for melanoma but also different tumor types and different irradiation sites and modalities using ICI and radiation as standard of care.

Among the T cell subsets, CD8 T cells play a central role in anti-tumor immunity, whereas Tregs contribute to the immunosuppressive capacity and dampen the anti-tumor immune response. Consequently, increased ratios of Tregs over CD8 T cells within the tumor microenvironment are one of the major factors which facilitate immune evasion and tumor growth<sup>38–41,42</sup>. In our study, patients treated in the Rad-ICI group showed reduced Treg activity, with no significant increases induced after radiation and ipi-based ICI therapy, while in the ICI-Rad group, Tregs were activated after the first dose of ICI already. Even though, in the Rad-ICI group, more patients were treated with ipi-nivo combination therapy, which might suppress activation of Treg, this might be a radiation-induced effect also. Accordingly, the Lasso analysis showed the change in numbers of activated Tregs over baseline Tregs in the patients' blood had the greatest influence on progression, whereas the rate of change in numbers of activated CD8 T cells over baseline Tregs was one of the best parameters associated with disease control. Targeting Tregs in combination with ICIs could overcome Treg-mediated resistance and increase the sensitivity of tumor cells to therapy, thereby enhancing tumor regression. Several clinical trials are underway to examine the therapeutic efficacy of different ICI combinations exceeding the ipi-nivo combination<sup>43,44</sup>. Interestingly, another significant parameter in the Lasso analysis associated with non-progression was the number of CD45RA-memory T cells. In line with this, Wistuba-Hamprecht et al. found a correlation of high frequencies of CD8+ effector memory T cells at baseline with response to ipilimumab and OS<sup>45</sup>. This might give the impression that these are mainly melanoma-specific, but this has not been investigated yet. In addition to the analysis of defined immune cell subsets, analyzing immune signatures consisting of several markers<sup>46</sup> or using radiomic-based signatures such as the CD8 T-cells associated radiomics signature described<sup>47</sup> might give further insights and help to understand the influence of RIT sequences on the immune response<sup>46</sup>.

This study was performed as an exploratory study and provides a rationale for combining RT with ICI therapy with a possible superiority for sequences starting with radiation followed by ICI therapy. However, there are many limitations associated with the study. Firstly, the limited number of patients in each treatment group and the non-randomized nature reduced the validity of statistical analyses. Also, the study covered a long time span with subsequent changes in standard of care. This resulted in the heterogeneity of patients between the groups and novel sub-groups, limiting statistical analyses. In addition, the impact of this study is reduced by the lack of examination of the tumor microenvironment (TME). As a result, we do not have insight into how RT may influence the immune landscape of TME based on the timing of the RIT sequence. Nevertheless, our current study contributes to increasing evidence that sequencing RT followed by ICI treatment may have better effects on the immunological tumor response and clinical outcomes

of patients with MBM. Still, larger clinical studies to validate this are necessary.

## Acknowledgments

The authors would like to thank all the patients and their families for their contribution to this study. Preliminary data of this work has been previously presented as a poster/abstract at ASCO 2019 (#e14104). Graphical representation was created using Biorender.

## Author contributions

JCH, JD, and PB conceived and designed the overall study. TES, MS, CM, KL, LK, MFH, AE, and JD collected and reviewed clinical data. IH performed sample processing and flow cytometry analysis. HS and JM performed ELISPOT analysis. JCH, TES, HS, MS, DM, CM, KL, LK, CK, RS, and PB analyzed and interpreted the data. MS, TES, DM, JCH prepared the original manuscript. All authors reviewed and approved the final manuscript.

## Data availability statement

The authors confirm that the data supporting the findings of this study are available within the article [and/or] its supplementary materials.

## Disclosure statement

TES, HS, JM, DM, KL, MFH, IH, CK, RS, and PB declare no competing interests. JCH received scientific grant support from BMS; honoraria for talks from Almirall, Amgen, BMS, GSK, MSD, Novartis, Pfizer, Pierre Fabre, Roche, Sanofi; advisory board member for MSD, Pierre Fabre; travel grants from BMS, Immunocore, 4SC. MS received honoraria for talks from Novartis; travel grants from Merck, Abbvie, Novartis, Sanofi-Aventis, BMS, Merck Sharp & Dome, Pfizer. CM received a fellowship from the German Research Foundation (DFG) (ME 5482/1-1) 2/2020-5/2021. LK reports personal fees from Accuray Inc., and Novocure GmbH. AE received honoraria for Biotest AG, Meet the Experts, Janssen-Cilag, Klinikum Minden; consulting fees for Biotest AG, MSD, Galderma Laboratorium, Janssen-Cilag, Roche, AbbVie; advisory board member for MSD, Biotest. JD received grants from Viewray Inc, Accuray International Sari, RaySearch Laboratories AB, Vision RT Limited, Astellas Pharma GmbH, Siemens Healthcare GmbH, Solution Akademie GmbH, Egomed PLC Surrey Research Park, Quintiles GmbH, Pharmaceutical Research Associates GmbH, Boehringer Ingelheim Pharma GmbH&CoKG, PTW-Freiburg Dr. Pychlau GmbH, Nanobiotix S.A., Accuray Incorporated.

## Funding

This study was supported by a Research Grant from Bristol Myers Squibb [CA184-436].

## Study approval

All patients declared written informed consent before study procedures. The study was approved by the ethical committee of the Medical Faculty of Heidelberg (S-246/2012).

## References

1. Davies MA, Liu P, McIntyre S, Kim KB, Papadopoulos N, Hwu W-J, Hwu P, Bedikian A. Prognostic factors for survival in melanoma patients with brain metastases. *Cancer*. 2011;117(8):1687–1696. published Online First: 2010/10/21. doi:10.1002/cncr.25634.

2. Patel JK, Didolkar MS, Pickren JW, Moore RH. Metastatic pattern of malignant melanoma. A study of 216 autopsy cases. *Am J Surg.* 1978;135(6):807–810. published Online First: 1978/06/01. doi:10.1016/0002-9610(78)90171-x.
3. Tawbi HA, Forsyth PA, Algazi A, Hamid O, Hodi FS, Moschos SJ, Khushalani NI, Lewis K, Lao CD, Postow MA, et al. Combined nivolumab and ipilimumab in melanoma metastatic to the brain. *The New England Journal of Medicine.* 2018;379(8):722–730. doi:10.1056/NEJMoa1805453.
4. Wolchok JD, Chiarion-Sileni V, Gonzalez R, Rutkowski P, Grob J-J, Cowey CL, Lao CD, Wagstaff J, Schadendorf D, Ferrucci PF, et al. Overall survival with combined nivolumab and ipilimumab in advanced melanoma. *N Engl J Med.* 2017;377(14):1345–1356. published Online First: 2017/09/12. doi:10.1056/NEJMoa1709684.
5. Kluger HM, Chiang V, Mahajan A, Zito CR, Sznol M, Tran T, Weiss SA, Cohen JV, Yu J, Hegde U, et al. Long-Term survival of patients with melanoma with active brain metastases treated with pembrolizumab on a phase II Trial. *J Clin Oncol.* 2019;37(1):52–60. [published Online First: 2018/11/09]. doi:10.1200/jco.18.00204.
6. Larkin J, Chiarion-Sileni V, Gonzalez R, Grob JJ, Cowey CL, Lao CD, Schadendorf D, Dummer R, Smylie M, Rutkowski P, et al. Combined nivolumab and ipilimumab or monotherapy in untreated melanoma. *N Engl J Med.* 2015;373(1):23–34. doi:10.1056/NEJMoa1504030.
7. Golden EB, Frances D, Pellicciotta I, Demaria S, Helen Barcellos-Hoff M, Formenti SC. Radiation fosters dose-dependent and chemotherapy-induced immunogenic cell death. *Oncoimmunology.* 2014;3(4):e28518. published Online First: 2014/07/30. doi:10.4161/onci.28518.
8. Pilonis KA, Vanpouille-Box C, Demaria S. Combination of radiotherapy and immune checkpoint inhibitors. *Semin Radiat Oncol.* 2015;25(1):28–33. [published Online First: 2014/12/08]. doi:10.1016/j.semradonc.2014.07.004.
9. Gulley JL, Arlen PM, Bastian A, Morin S, Marte J, Beetham P, Tsang K-Y, Yokokawa J, Hodge JW, Ménard C, et al. Combining a recombinant cancer vaccine with standard definitive radiotherapy in patients with localized prostate cancer. *J Clin Cancer Res.* 2005;11(9):3353–3362. doi:10.1158/1078-0432.CCR-04-2062.
10. Vanpouille-Box C, Formenti SC, Demaria S. Toward precision radiotherapy for use with immune checkpoint blockers. *Clin Cancer Res.* 2018;24(2):259–265. [published Online First: 2017/07/29]. doi:10.1158/1078-0432.Ccr-16-0037.
11. Teng F, Kong L, Meng X, Yang J, Yu J. Radiotherapy combined with immune checkpoint blockade immunotherapy: achievements and challenges. *Cancer Lett.* 2015;365(1):23–29. [published Online First: 2015/05/20]. doi:10.1016/j.canlet.2015.05.012.
12. Topalian SL, Hodi FS, Brahmer JR, Gettinger SN, Smith DC, McDermott DF, Powderly JD, Carvajal RD, Sosman JA, Atkins MB, et al. Safety, activity, and immune correlates of Anti-PD-1 antibody in cancer. *New Engl J Med.* 2012;366(26):2443–2454. doi:10.1056/NEJMoa1200690.
13. Formenti SC, Demaria S. Combining radiotherapy and cancer immunotherapy: a paradigm shift. *J Natl Cancer Inst.* 2013;105(4):256–265. [published Online First: 2013/01/08]. doi:10.1093/jnci/djs629.
14. Dovedi SJ, Adlard AL, Lipowska-Bhalla G, McKenna C, Jones S, Cheadle EJ, Stratford IJ, Poon E, Morrow M, Stewart R, et al. Acquired resistance to fractionated radiotherapy can be overcome by concurrent PD-L1 blockade. *Cancer Res.* 2014;74(19):5458–5468. [published Online First: 2014/10/03]. doi:10.1158/0008-5472.CAN-14-1258.
15. Syn NL, Teng MWL, Mok TSK, Soo RA. De-novo and acquired resistance to immune checkpoint targeting. *Lancet Oncol.* 2017;18(12):e731–e41. [published Online First: 2017/12/07]. doi:10.1016/S1470-2045(17)30607-1.
16. Persa E, Balogh A, Safrany G, Lumniczky K. The effect of ionizing radiation on regulatory T cells in health and disease. *Cancer Lett.* 2015;368(2):252–261. [published Online First: 2015/03/11]. doi:10.1016/j.canlet.2015.03.003.
17. Demaria S, Kawashima N, Yang AM, Devitt ML, Babb JS, Allison JP, Formenti SC. Immune-mediated inhibition of metastases after treatment with local radiation and CTLA-4 blockade in a mouse model of breast cancer. *Clin Cancer Res.* 2005;11(2 Pt 1):728–734. [published Online First: 2005/02/11].
18. Yoshimoto Y, Suzuki Y, Mimura K, Ando K, Oike T, Sato H, Okonogi N, Maruyama T, Izawa S, Noda S-E, et al. Radiotherapy-induced anti-tumor immunity contributes to the therapeutic efficacy of irradiation and can be augmented by CTLA-4 blockade in a mouse model. *PLoS One.* 2014;9(3):e92572. [published Online First: 2014/04/02]. doi:10.1371/journal.pone.0092572.
19. Twyman-Saint Victor C, Rech AJ, Maita A, Rengan R, Pauken KE, Stelekati E, Benci JL, Xu B, Dada H, Odorizzi PM, et al. Radiation and dual checkpoint blockade activate non-redundant immune mechanisms in cancer. *Nature.* 2015;520(7547):373–377. [published Online First: 2015/03/11]. doi:10.1038/nature14292.
20. Spitzer MH, Carmi Y, Reticker-Flynn NE, Kwek SS, Madhiredy D, Martins MM, Gherardini PF, Prestwood TR, Chabon J, Bendall SC, et al. Systemic immunity is required for effective cancer immunotherapy. *Cell.* 2017;168(3):487–502.e15. published Online First: 2017/01/24. doi:10.1016/j.cell.2016.12.022.
21. Chow J, Hoffend NC, Abrams SI, Schwaab T, Singh AK, Muhitch JB. Radiation induces dynamic changes to the T cell repertoire in renal cell carcinoma patients. *J Proc National Acad Sci.* 2020;117(38):23721–23729. doi:10.1073/pnas.2001933117.
22. Eisenhauer EA, Therasse P, Bogaerts J, Schwartz LH, Sargent D, Ford R, Dancy J, Arbuck S, Gwyther S, Mooney M, et al. New response evaluation criteria in solid tumours: revised RECIST guideline (version 1.1). *Eur J Cancer.* 2009;45(2):228–247. [published Online First: 2008/12/23]. doi:10.1016/j.ejca.2008.10.026.
23. Schmitz-Winnenthal FH, Hohmann N, Schmidt T, Podola L, Friedrich T, Lubenau H, Springer M, Wiecekowski S, Breiner KM, Mikus G, et al. A phase I trial extension to assess immunologic efficacy and safety of prime-boost vaccination with VX001, an oral T cell vaccine against VEGFR2, in patients with advanced pancreatic cancer. *Oncoimmunology.* 2018;7(4):e1303584. [published Online First: 2018/04/11]. doi:10.1080/2162402x.2017.1303584.
24. Pfirschke C, Gebhardt C, Zörnig I, Pritsch M, Eichmüller SB, Jäger D, Enk A, Beckhove P. T cell responses in early-stage melanoma patients occur frequently and are not associated with humoral response. *Cancer Immunol Immunother.* 2015;64(11):1369–1381. [published Online First: 2015/07/15]. doi:10.1007/s00262-015-1739-8.
25. Friedman JH, Hastie T, Tibshirani R. Regularization paths for generalized linear models via coordinate descent. *J J Stat Software.* 2010;33(1):22. [published Online First: 2010-02-02]. doi:10.18637/jss.v033.i01.
26. R Core Team. R: A language and environment for statistical computing. Vienna, Austria: R Foundation for Statistical Computing; 2019. <https://www.R-project.org/>.
27. McGee HM, Daly ME, Azghadi S, Stewart SL, Oesterich L, Schlom J, Donahue R, Schoenfeld JD, Chen Q, Rao S, et al. Stereotactic ablative radiation therapy induces systemic differences in peripheral blood immunophenotype dependent on irradiated site. *Int J Radiat Oncol Biol Phys.* 2018;101(5):1259–1270. [published Online First: 2018/06/13]. doi:10.1016/j.ijrobp.2018.04.038.
28. Kalia V, Yuzefpolskiy Y, Vegaraju A, Xiao H, Baumann F, Jatav S, Church C, Prlic M, Jha A, Nghiem P, et al. Metabolic regulation by PD-1 signaling promotes long-lived quiescent CD8 T cell memory in mice. *Sci Transl Med.* 2021;13(615):eaba6006. [published Online First: 2021/10/14]. doi:10.1126/scitranslmed.aba6006.
29. Kiess AP, Wolchok JD, Barker CA, Postow MA, Tabar V, Huse JT, Chan TA, Yamada Y, Beal K. Stereotactic radiosurgery for melanoma brain metastases in patients receiving ipilimumab: safety profile and efficacy of combined treatment. *Int J Radiat Oncol Biol Phys.* 2015;92(2):368–375. [published Online First: 2015/03/11]. doi:10.1016/j.ijrobp.2015.01.004.
30. An Y, Jiang W, Kim BYS, Qian JM, Tang C, Fang P, Logan J, D'Souza NM, Haydu LE, Wang XA, et al. Stereotactic radiosurgery of early melanoma brain metastases after initiation of anti-CTLA-4

- treatment is associated with improved intracranial control. *Radiother oncol.* 2017;125(1):80–88. [published Online First: 2017/09/17]. doi:10.1016/j.radonc.2017.08.009.
31. Schoenfeld JD, Mahadevan A, Floyd SR, Dyer MA, Catalano PJ, Alexander BM, McDermott DF, Kaplan ID. Ipilimumab and cranial radiation in metastatic melanoma patients: a case series and review. *J Immunother Cancer.* 2015;3:50. [published Online First: 2015/12/18]. doi:10.1186/s40425-015-0095-8.
  32. Patel KR, Shoukat S, Oliver DE, Chowdhary M, Rizzo M, Lawson DH, Khosa F, Liu Y, Khan MK. Ipilimumab and stereotactic radiosurgery versus stereotactic radiosurgery alone for newly diagnosed melanoma brain metastases. *Am J Clin Oncol.* 2017;40(5):444–450. [published Online First: 2015/05/29]. doi:10.1097/coc.000000000000199.
  33. Skrepnik T, Sundararajan S, Cui H, Stea B. Improved time to disease progression in the brain in patients with melanoma brain metastases treated with concurrent delivery of radiosurgery and ipilimumab. *Oncoimmunology.* 2017;6(3):e1283461. [published Online First: 2017/04/14]. doi:10.1080/2162402x.2017.1283461.
  34. Schmidberger H, Rapp M, Ebersberger A, Hey-Koch S, Loquai C, Grabbe S, Mayer A. Long-term survival of patients after ipilimumab and hypofractionated brain radiotherapy for brain metastases of malignant melanoma: sequence matters. *Strahlenther Onkol.* 2018;194(12):1144–1151. [published Online First: 2018/10/10]. doi:10.1007/s00066-018-1356-5.
  35. Rauschenberg R, Bruns J, Brutting J, Daubner D, Lohaus F, Zimmer L, Forschner A, Zips D, Hassel JC, Berking C, et al. Impact of radiation, systemic therapy and treatment sequencing on survival of patients with melanoma brain metastases. *Eur J Cancer.* 2019;110:11–20. [published Online First: 2019/02/12]. doi:10.1016/j.ejca.2018.12.023.
  36. Fu T, He Q, Sharma P. The ICOS/ICOSL pathway is required for optimal antitumor responses mediated by Anti-CTLA-4 therapy. *J Cancer Res.* 2011;71(16):5445–5454. doi:10.1158/0008-5472.CAN-11-1138.
  37. Shaverdian N, Lisberg AE, Bornazyan K, Veruttipong D, Goldman JW, Formenti SC, Garon EB, Lee P. Previous radiotherapy and the clinical activity and toxicity of pembrolizumab in the treatment of non-small-cell lung cancer: a secondary analysis of the KEYNOTE-001 phase 1 trial. *Lancet Oncol.* 2017;18(7):895–903. [published Online First: 2017/05/30]. doi:10.1016/S1470-2045(17)30380-7.
  38. Peng L-S, Zhuang Y, Shi Y, Zhao Y-L, Wang -T-T, Chen N, Cheng P, Liu T, Liu X-F, Zhang J-Y, et al. Increased tumor-infiltrating CD8+Foxp3+ T lymphocytes are associated with tumor progression in human gastric cancer. *Cancer Immunol Immunother.* 2012;61(11):2183–2192. [published Online First: 2012/06/26]. doi:10.1007/s00262-012-1277-6.
  39. Yoon HH, Orrock JM, Foster NR, Sargent DJ, Smyrk TC, Sinicrope FA. Prognostic impact of FoxP3+ regulatory T cells in relation to CD8+ T lymphocyte density in human colon carcinomas. *PLoS One.* 2012;7(8):e42274. [published Online First: 2012/08/11]. doi:10.1371/journal.pone.0042274.
  40. deLeeuw RJ, Kost SE, Kakal JA, Nelson BH. The prognostic value of FoxP3+ tumor-infiltrating lymphocytes in cancer: a critical review of the literature. *Clin Cancer Res.* 2012;18(11):3022–3029. [published Online First: 2012/04/19]. doi:10.1158/1078-0432.Ccr-11-3216.
  41. Nishikawa H, Sakaguchi S. Regulatory T cells in cancer immunotherapy. *Curr Opin Immunol.* 2014;27:1–7. [published Online First: 2014/01/15]. doi:10.1016/j.coi.2013.12.005.
  42. Robert L, Harview C, Emerson R, Wang X, Mok S, Homet B, Comin-Anduix B, Koya RC, Robins H, Tumeh PC, et al. Distinct immunological mechanisms of CTLA-4 and PD-1 blockade revealed by analyzing TCR usage in blood lymphocytes. *Oncoimmunology.* 2014;3:e29244. [published Online First: 2014/08/02]. doi:10.4161/onci.29244.
  43. Sasidharan Nair V, Elkord E. Immune checkpoint inhibitors in cancer therapy: a focus on T-regulatory cells. *Immunol Cell Biol.* 2018;96(1):21–33. [published Online First: 2018/01/24]. doi:10.1111/imcb.1003.
  44. Jenkins RW, Barbie DA, Flaherty KT. Mechanisms of resistance to immune checkpoint inhibitors. *Br J Cancer.* 2018;118(1):9–16. doi:10.1038/bjc.2017.434.
  45. Wistuba-Hamprecht K, Martens A, Heubach F, Romano E, Geukes Foppen M, Yuan J, Postow M, Wong P, Mallardo D, Schilling B, et al. Peripheral CD8 effector-memory type 1 T-cells correlate with outcome in ipilimumab-treated stage IV melanoma patients. *Eur J Cancer.* 2017;73:61–70. [published Online First: 2017/02/09]. doi:10.1016/j.ejca.2016.12.011.
  46. Zhou JG, Donaubaue AJ, Frey B, Becker I, Rutzner S, Eckstein M, Sun R, Ma H, Schubert P, Schweizer C, et al. Prospective development and validation of a liquid immune profile-based signature (LIPS) to predict response of patients with recurrent/metastatic cancer to immune checkpoint inhibitors. *J Immunother Cancer.* 2021;9(2). [published Online First: 2021/02/18]. doi:10.1136/jitc-2020-001845.
  47. Sun R, Sundahl N, Hecht M, Putz F, Lancia A, Rouyar A, Milic M, Carré A, Battistella E, Alvarez Andres E, et al. Radiomics to predict outcomes and absopal response of patients with cancer treated with immunotherapy combined with radiotherapy using a validated signature of CD8 cells. *J Immunother Cancer.* 2020;8(2):e001429. [published Online First: 2020/11/15]. doi:10.1136/jitc-2020-001429.